1   **Flexpart v10.1 simulation of source contributions to Arctic black carbon**

3   Chunmao Zhu[1], Yugo Kanaya[1,2], Masayuki Takigawa[1,2], Kohei Ikeda[3], Hiroshi Tanimoto[3],

4   Fumikazu Taketani[1,2], Takuma Miyakawa[1,2], Hideki Kobayashi[1,2], Ignacio Pisso[4]

6   [1]Research Institute for Global Change, Japan Agency for Marine–Earth Science and

7   Technology (JAMSTEC), Yokohama 2360001, Japan

8   [2]Institute of Arctic Climate and Environmental Research, Japan Agency for Marine–Earth

9   Science and Technology, Yokohama 2360001, Japan

10   [3]National Institute for Environmental Studies, Tsukuba 305-8506, Japan

11   [4]NILU – Norwegian Institute for Air Research, Kjeller 2027, Norway

13   Correspondence to Chunmao Zhu (chmzhu@jamstec.go.jp)

14   **Abstract**

15   The Arctic environment is undergoing rapid changes such as faster warming than the

16   global average and exceptional melting of glaciers in Greenland. Black carbon (BC) particles,

17   which are a short-lived climate pollutant, are one cause of Arctic warming and glacier

18   melting. However, the sources of BC particles are still uncertain. We simulated the potential

19   emission sensitivity of atmospheric BC present over the Arctic (north of 66° N) using the

20   Flexpart Lagrangian transport model (version 10.1). This version includes a new aerosol wet

21   removal scheme, which better represents particle-scavenging processes than older versions

22   did. Arctic BC at the surface (0–500 m) and high altitudes (4750–5250 m) is sensitive to

23   emissions in high latitude (north of 60° N) and mid-latitude (30–60° N) regions, respectively.

24   Geospatial sources of Arctic BC were quantified, with a focus on emissions from

25   anthropogenic activities and biomass burning in 2010. We found that anthropogenic sources

26   contributed 82 % and 83 % of annual Arctic BC at the surface and high altitudes,

27   respectively. Arctic surface BC comes predominantly from anthropogenic emissions in

28   Russia (56 %), with gas flaring from the Yamalo-Nenets Autonomous Okrug and Komi

29   Republic being the main source (31 % of Arctic surface BC). These results highlight the need

30   for regulations to control BC emissions from gas flaring to mitigate the rapid changes in the

31   Arctic environment. In summer, combined biomass burning in Siberia, Alaska, and Canada

32   contributes 56–85 % (75 % on average) and 40–72 % (57 %) of Arctic BC at the surface and

33   high altitudes, respectively. A large fraction (40 %) of BC in the Arctic at high altitudes comes

34   from anthropogenic emissions in East Asia, which suggests that the rapidly growing

35   economies of developing countries could have a non-negligible effect on the Arctic. To our

36   knowledge, this is the first year-round evaluation of Arctic BC sources that has been

37   performed using the new wet deposition scheme in Flexpart. The study provides a scientific

38   basis for actions to mitigate the rapidly changing Arctic environment.

39

1 Introduction

The Arctic region has experienced warming at a rate twice that of the global average in recent decades (Cohen et al., 2014). The Arctic cryosphere has been undergoing unprecedented changes since the mid-1800s (Trusel et al., 2018). Glacier cover in Greenland reached its historically lowest level in summer 2012 (Tilling et al., 2015). Evidence indicates that the emissions and transport of greenhouse gases and aerosols to the Arctic region are contributing to such warming and melting of snow and ice (Keegan et al., 2014; Najafi et al., 2015). Short-lived climate pollutants such as black carbon (BC) particles, tropospheric ozone, and methane greatly affect the Arctic climate (AMAP, 2015; Quinn et al., 2008).

BC particles are emitted during incomplete combustion of fossil fuels, biofuels, and biomass. BC warms the atmosphere by direct absorption of solar radiation. The deposition of BC on snow and ice surfaces accelerates their melting through decreasing albedo, which contributes to the rapid loss of glaciers. In the Arctic region, ground-based observations have indicated that BC shows clear seasonal variations, with elevated mass concentrations in winter and spring (the so-called Arctic haze) and low values in summer (Law and Stohl, 2007). Such seasonal variations are explained by increased transport from lower latitudes in the cold season and increased wet scavenging in the warm season (Shaw, 1995; Garrett et al., 2011; Shen et al., 2017).

The presence of BC particles in the Arctic is mainly attributed to emissions in high-latitude regions outside the Arctic, such as northern Europe and Russia (Stohl, 2006; Brock et al., 2011). This is partly caused by the polar dome (Stohl, 2006), which is formed because of the presence of constant potential temperature near the surface. The emissions in high-latitude regions are transported to the Arctic region and trapped in the dome, which increases the surface concentration. Recently, Schmale et al. (2018) suggested that local emissions from

64   within the Arctic are another important source, and these are expected to increase in the

65   future.

66   Although numerous studies have been performed, results regarding regional

67   contributions of BC sources in the Arctic are still inconclusive. For example, ground-based

68   observations and Lagrangian transport model results reported by Winiger et al. (2016)

69   showed that BC in Arctic Scandinavia is predominantly linked to emissions in Europe. Over

70   the whole Arctic region (north of 66° N), Russia contributes 62 % to surface BC in terms of

71   the annual mean (Ikeda et al., 2017). Gas flaring in Russia has been identified as a major

72   (42 %) source of BC at the Arctic surface (Stohl et al., 2013). Xu et al. (2017) found that

73   anthropogenic emissions from northern Asia contribute 40–45 % of Arctic surface BC in

74   winter and spring. However, the results of some other studies have suggested that Russia,

75   Europe, and South Asia each contribute 20–25 % of BC to the low-altitude springtime Arctic

76   haze (Koch and Hansen, 2005). Sand et al. (2016) found that the surface temperature in the

77   Arctic is most sensitive to emissions in Arctic countries, and Asian countries contribute

78   greatly to Arctic warming because of the large absolute amount of emissions.

79   Various models have been used to investigate BC sources in the Arctic. Depending on the

80   simulation method, these models are generally categorized as Lagrangian transport models

81   (Hirdman et al., 2010; Liu et al., 2015; Stohl et al., 2006, 2013), chemical transport models

82   (Ikeda et al., 2017; Koch and Hansen, 2005; Qi et al., 2017; Shindell et al., 2008; Wang et al.,

83   2011; Xu et al., 2017), and global climate models (Ma et al., 2013; Schacht et al., 2019; H.

84   Wang et al., 2014). The uncertainties of the simulations are mainly generated from the

85   model treatment of processes for BC particle removal, especially wet-scavenging processes

86   (Kipling et al., 2013; Schacht et al., 2019; Q. Wang et al., 2014). The use of emission

87   inventories is another important factor that affects the simulation results (Dong et al.,

88   2019). The observations of BC that are used for model comparisons may be biased by 30 %

89   depending on the method used (Sinha et al., 2017; Sharma et al., 2017). There are still large

90   uncertainties regarding the sources of BC in the Arctic with respect to emission sectors

91   (anthropogenic sources and biomass burning) and geospatial contributions (Eckhardt et al.,

92   2015).

93   In this study, we quantified region-separated sources of BC in the Arctic in 2010 by using

94   version 10.1 of the FLEXible PARTicle dispersion model (Flexpart) (Stohl et al., 1998, 2006,

95   2013; Grythe et al., 2017). We first evaluated the model performance by comparing the

96   results with those based on observations at surface sites. The source contributions of

97   emission sectors and geospatial contributions were evaluated by incorporating the Arctic BC

98   footprint into the emission inventories.

2   Materials and methods

99

100   2.1 Transport model

101   The Flexpart model (version 10.1) was run in backward mode to simulate BC footprints in

102   the Arctic region. The calculation of wet deposition was improved compared with those in

103   previous versions because in-cloud scavenging and below-cloud scavenging of particles were

104   separately calculated (Grythe et al., 2017). In previous versions of Flexpart, in the in-cloud

105   scavenging scheme, the aerosol scavenging coefficient depended on the cloud water

106   content, which was calculated according to an empirical relationship with precipitation rate,

107   in which all aerosols had the same nucleation efficiency (Hertel et al., 1995 ; Stohl et al.,

108   2005). In the new version, the in-cloud scavenging scheme depends on the cloud water

109   phase (liquid, ice, or mixed phase). Aerosols were set as ice nuclei for ice clouds and as

110   cloud condensation nuclei for liquid-water clouds, respectively. For mixed-phase clouds, it

111   was assumed that 10 % of aerosols are ice nuclei and 90 % are cloud condensation nuclei,

112   because BC is much more efficiently removed in liquid water clouds than in ice clouds (Cozic

113   et al., 2007; Grythe et al., 2017). The below-cloud scavenging scheme can parameterize

114   below-cloud removal as a function of aerosol particle size, and precipitation type (snow or

115   rain) and intensity. The biases produced in simulations using the new scheme are therefore

116   smaller than those in the old scheme for wet deposition of aerosols, especially at high

117   latitudes (Grythe et al., 2017).

118   The Arctic region is defined as areas north of 66° N. The potential BC emission

119   sensitivities at two heights in the Arctic region, i.e., the surface (0–500 m) and 5000 m

120   (4750–5250 m), were simulated. The Flexpart outputs were set as gridded retention times.

121   We performed tests at 500, 2000, and 5000 m, and chose 500 m as the upper boundary

122   height of the model output. The model was driven with operational analytical data from the

123   European Centre for Medium-Range Weather Forecasts (ECMWF) at a spatial resolution of

124   1° × 1° with 61 vertical levels. Temporally, ECMWF has a resolution of 3 h, with 6 h analysis

125   and 3 h forecast time steps. The simulation period was set at 60 days backward starting

126   from each month in 2010. The maximum life time of BC was set at 20 days because its

127   suspension time in the upper atmosphere during long-range transport is longer than that at

128   the surface level (Stohl et al., 2013). We implemented the wet deposition scheme in the

129   backward calculations, but it was not represented in the default setting (Flexpart v10.1,

130   https://www.flexpart.eu/downloads, obtained 10 April 2017).

131   The chemistry and microphysics could not be resolved by Flexpart. The model therefore

132   ignores hydrophobic to hydrophilic state changes and size changes of BC, and assumes that

133   all BC particles are aged hydrophilic particles. A logarithmic size distribution of BC with a

134   mean diameter of 0.16 μm and a standard deviation of 1.96, in accordance with our ship

135   observations in the Arctic, was used (Taketani et al., 2016). The particle density was

136   assumed to be 2000 kg m⁻³, and 1 million computational particles were randomly generated

137   in the Arctic region for the backward runs.

138   Four ground-based observations made during the period 2007–2011 were used to

139   validate the model performance. The potential BC emission sensitivity at 0–500 m above

140   ground level from a 0.1° grid centered at each site was simulated. Other model

141   parameterizations were consistent with those for the Arctic region, except that 200 000

142   computational particles were released.

143   2.2 Emission inventories

144   We focused on BC sources from anthropogenic emissions and biomass burning. The

145   Hemispheric Transport of Air Pollution version 2 inventory (HTAP2) for 2010 was used for

146   anthropogenic emissions (Janssens-Maenhout et al., 2015). However, as it has been

147   reported that BC emissions in Russia were underestimated in HTAP2, we used the BC

148   emissions reported by Huang et al. (2015) for Russia, in which the annual BC emissions were

149   224 Gg yr⁻¹. For biomass burning, we used the Global Fire Emissions Database version 3

150   inventory (GFED3) (van der Werf et al., 2010) for the purposes of intercomparison with

151   other studies, as this version is widely used. Geospatial distributions of emissions from

152   anthropogenic sources and biomass burning in January and July are shown in Fig. S1.

153   2.3 Calculation of Arctic BC source contributions

154   The source contributions to Arctic BC were derived by incorporating the gridded

155   retention time into the column emission flux, which was derived from the emission

156   inventories in each grid. Calculations for anthropogenic sources and biomass burning were

157   performed separately and the sum was used. For anthropogenic sources, the regions were

158   separated into North America and Canada (25–80° N, 50–170° W), Europe (30–80° N, 0–30°

159   E), Russia (53–80° N, 30–180° E), East Asia (35–53° N, 75–150° E and 20–35° N, 100–150° E),

160   and others (the rest) (Fig. 1a). For biomass-burning sources, the regions were separated into

161   Alaska and Canada (50–75° N, 50–170° W), Siberia (50–75° N, 60–180° E), and others (Fig.

162   1b).

163   **3   Results and discussion**

164   **3.1. Comparisons of simulations with BC observations at Arctic surface sites**

165   BC levels simulated by Flexpart were compared with those based on surface observations

166   at four sites: Barrow, USA (156.6° W, 71.3° N, 11 m asl), Alert, Canada (62.3° W, 82.5° N,

167   210 m asl), Zeppelin, Norway (11.9° E, 78.9° N, 478 m asl), and Tiksi, Russia (128.9° E, 71.6°

168   N, 8 m asl). Aerosol light absorption was determined by using particle soot absorption

169   photometers (PSAPs) at Barrow, Alert, and Zeppelin, and an aethalometer at Tiksi. For PSAP

170   measurements, the equivalent BC values were derived using a mass absorption efficiency of

171   10 m^2 g^{-1}. The equivalent BC at Tiksi, which was determined with an aethalometer, was

172   obtained directly. These measurement data were obtained from the European Monitoring

173   and Evaluation Programme and World Data Centre for Aerosols database

174   (http://ebas.nilu.no).

175   It is worth noting that uncertainties could be introduced by using different BC

176   measurement techniques. An evaluation of three methods for measuring BC at Alert,

177   Canada indicated that an average of the refractory BC determined with a single-particle soot

178   photometer (SP2) and elemental carbon (EC) determined from filter samples give the best

179   estimate of BC mass (Sharma et al., 2017). Xu et al. (2017) reported that the equivalent BC

180   determined with a PSAP was close to the average of the values for refractory BC and EC at

181   Alert. In this study, we consider that the equivalent BC values determined with a PSAP at

182   Barrow, Alert, and Zeppelin to be the best estimate. There may be uncertainties in the

183   equivalent BC observations performed with an aethalometer at Tiksi because of co-existing

184 particles such as light-absorptive organic aerosols, scattering particles, and dusts

185 (Kirchstetter et al., 2004; Lack and Langridge, 2013). Interference by the filter and

186 uncertainties in the mass absorption cross section could also contribute to the bias

187 observed in measurements made with an aethalometer at Tiksi.

188   Flexpart generally reproduced the seasonal variations in BC at four Arctic sites well (Fig.

189 2). Winter maxima and summer minima were observed [Pearson correlation coefficient (R) =

190 0.53–0.80, root-mean-square error (RMSE) = 15.1–56.8 ng m^{-3}]. This seasonality is probably

191 related to relatively stronger transport to the Arctic region in winter, accompanied by lower

192 BC aging and inefficient removal, as simulated by older versions of Flexpart (Eckhardt et al.,

193 2015; Stohl et al., 2013). In the older versions of Flexpart, in which clouds were

194 parameterized based on relative humidity, clouds frequently extended to the surface and at

195 times no clouds could be found in grid cells, with unrealistic precipitation (Grythe et al.,

196 2017). In comparison, in Flexpart v10.1, in which cloud is differentiated into liquid, solid, and

197 mixed phase, the cloud distribution is more consistent with the precipitation data. This

198 improvement in the cloud distribution and phase leads to a more realistic distribution of

199 below-cloud and in-cloud scavenging events.

200   Flexpart v10.1 underestimated observed BC in January to May at Barrow and Alert, and in

201 most months at Tiksi. This is probably related to the emission inventory used, although

202 seasonal variations in residential heating are included in HTAP2, which would reduce the

203 simulation bias (Xu et al., 2017). Simulations by GEOS-Chem using the same emission

204 inventories also underestimated BC levels at Barrow and Alert (Ikeda et al., 2017; Xu et al.,

205 2017). At Zeppelin, the Flexpart-simulated BC was higher than the observed value, especially

206 in winter. It has been reported that riming in mixed-phase clouds occurs frequently at

207 Zeppelin (Qi et al., 2017). During the riming process, BC particles act as ice particles and

208   collide with the relatively numerous water drops, which form frozen cloud droplets, and

209   then snow is precipitated. This results in relatively efficient BC scavenging (Hegg et al.,

210   2011). Such a process could not be dealt with by the model.

211   Anthropogenic emissions are the main sources of BC at the four Arctic sites from late

212   autumn to spring, whereas biomass-burning emissions make large contributions in summer.

213   From October to April, anthropogenic emissions accounted for 87–100 % of BC sources at all

214   the observation sites. At Barrow, biomass burning accounted for 54–86 % of BC in June–

215   September (Fig. 2a). It was reported that observed high values of BC were unintentionally

216   excluded by local pollution data screening from the data set for Barrow in the forest fire

217   season in summer (Stohl et al., 2013); the notably higher level of simulated BC may reflect

218   this. There are large interannual variations in both observed and simulated BC (Fig. S2). In

219   June–August 2010, the mean contributions of biomass burning to BC were ~9.8, 6.3, 2.4,

220   and 8.6 times those from anthropogenic sources at Barrow, Alert, Zeppelin, and Tiksi,

221   respectively. In this study, we focused on BC in the Arctic region in 2010.

222   **3.2 Potential emission sensitivity of Arctic BC**

223   The potential emission sensitivities (footprint) of Arctic BC showed different patterns

224   with respect to altitude. The Arctic surface is sensitive to emissions at high latitudes (>60°

225   N). Air masses stayed for over 60 s in each of the 1° grids from the eastern part of northern

226   Eurasia and the Arctic Ocean before being transported to the Arctic surface in the winter,

227   represented by January (Fig. 3a). In comparison, during the summer, represented by July, BC

228   at the Arctic surface was mainly affected by air masses that originated from the Arctic

229   Ocean and the Norwegian Sea (Fig. 3b). These results imply that local BC emissions within

230   the Arctic regions, although relatively weak compared with those from the mid-latitude

231   regions, could strongly affect Arctic air pollution. Local BC emissions are important in the

232   wintertime because the relatively stable boundary layer does not favor pollution dispersion.

233   Recent increases in anthropogenic emissions in the Arctic region, which have been caused

234   by the petroleum industry and development of the Northern Sea Route, are expected to

235   cause deterioration of air quality in the Arctic. Socio-economic developments in the Arctic

236   region would increase local BC emissions, and this will be a non-negligible issue in the future

237   (Roiger et al., 2015; Schmale et al., 2018).

238   BC at high altitudes (~ 5000 m) in the Arctic is more sensitive to mid-latitude (30–60° N)

239   emissions, especially in wintertime. In January, air masses hovered over the Bering Sea and

240   the North Atlantic Ocean before arriving at the Arctic (Fig. 3c). A notable corridor at 30–50°

241   N covering Eurasia and the United States was the sensitive region that affected BC at high

242   altitudes in the Arctic in January. These results indicate that mid-latitude emissions,

243   especially those with relatively large strengths from East Asia, East America, and Europe,

244   could alter the atmospheric constituents at high altitudes in the Arctic. Central to east

245   Siberia was the most sensitive region for BC at high altitudes in the Arctic in July (Fig. 3d).

246   These results suggest that pollutants from frequent and extensive wildfires in Siberia in

247   summer are readily transported to high altitudes in the Arctic. Boreal fires are expected to

248   occur more frequently and over larger burning areas under future warming (Veira et al.,

249   2016), therefore the atmospheric constituents and climate in the Arctic could undergo more

250   rapid changes.

251   **3.3 Seasonal variations and sources of Arctic surface BC**

252   Arctic surface BC showed clear seasonal variations, with a primary peak in winter–spring

253   (December–March, 61.8–82.8 ng m^{-3}) and a secondary peak in summer (July, 52.7 ng m^{-3}).

254   BC levels were relatively low in May–June (21.8–23.1 ng m^{-3}) and September–November

255   (34.1–40.9 ng m^{-3}) (Fig. 4a). This seasonality is in agreement with observations and

256   simulations at Arctic sites (Barrow, Alert, and Tiksi) (Stohl et al., 2013), and previous studies

257   targeting the whole Arctic (Ikeda et al., 2017; Xu et al., 2017). Compared with the study

258   reported by Stohl et al. (2013), the current work using the new scheme produced smaller

259   discrepancies between the simulated data and observations. Although the simulation

260   periods (monthly means for 2007–2011 in this study and for 2008–2010 in the old scheme)

261   and the anthropogenic emission inventories (HTAP2 in this study and ECLIPSE4 in the

262   previous study) are different, the new scheme shows potential for better representing BC

263   transport and removal processes in the Arctic.

264   The annual mean Arctic BC at the surface was estimated to be 48.2 ng m^{-3}. From October

265   to April, anthropogenic sources accounted for 96–100 % of total BC at the Arctic surface.

266   Specifically, anthropogenic emissions from Russia accounted for 61–76 % of total BC in

267   October–May (56 % annually), and was the dominant sources of Arctic BC at the surface.

268   From an isentropic perspective, the meteorological conditions in winter favored the

269   transport of pollutants from northern Eurasia to the lower Arctic, along with diabatic cooling

270   and strong inversions (Klonecki et al., 2003). In comparison, biomass burning from boreal

271   regions accounted for 56–85 % (75 % on average) of Arctic BC at the surface in summer;

272   biomass-burning emissions from North America and Canada accounted for 54 % of total

273   Arctic surface BC in June, and those from Siberia accounted for 59–61 % in July–August.

274   Wildfires in the boreal forests in summer had a major effect on air quality in the Arctic. On

275   an annual basis, anthropogenic sources and biomass-burning emissions accounted for 82 %

276   and 18 %, respectively, of total Arctic surface BC. In comparison, a recent study based on

277   isotope observations at the Arctic sites and a Flexpart model simulation suggested that

278   biomass burning contributed 39 % of annual BC in 2011–2015 (Winiger et al., 2019).

279   The geospatial contributions of anthropogenic sources and biomass-burning emissions

280   can be further illustrated by taking January and July as examples. In January, high levels of

281   anthropogenic emissions from Russia (contributing 64 % of Arctic surface BC), Europe

282   (18 %), and East Asia (9 %) were identified (Fig. 5a). Specifically, Yamalo-Nenets

283   Autonomous Okrug in Russia, which has the largest reserves of Russia's natural gas and oil

284   (Filimonova et al., 2018), was the most notable emission hotspot, which suggests gas-flaring

285   sources. The Komi Republic in Russia was also identified as a strong anthropogenic emitter

286   contributing to Arctic surface BC. These gas-flaring industrial regions in Russia (58–69° N,

287   68–81°E) together contributed 33 % and 31 % of Arctic surface BC for January and the

288   annual mean, respectively. Recently, Dong et al. (2019) evaluated BC emission inventories

289   using GEOS-Chem and proposed that using the inventory compiled by Huang et al. (2015)

290   for Russia, in which gas flaring accounted for 36 % of anthropogenic emissions, had no

291   prominent impact on the simulation performance in Russia and the Arctic. They suggested

292   that use of a new global inventory for BC emissions from natural gas flaring would improve

293   the model performance (Huang and Fu, 2016). These results suggest that inclusion of BC

294   emissions from gas flaring on the global scale is necessary for further BC simulations.

295   In Europe, a relatively high contribution of anthropogenic emissions to Arctic surface BC

296   in January was made by Poland (50–55° N, 15–24° E, contributing 4 % of Arctic surface BC)

297   because of relatively large emission fluxes in the region (Fig. S1a). Anthropogenic emissions

298   from East China, especially those north of ~33° N (33–43° N, 109–126° E), contributed

299   perceptibly (5 %) to Arctic surface BC.

300   In July, contributions from anthropogenic sources shrank to those from Yamalo-Nenets

301   Autonomous Okrug and Komi Republic in Russia, and contributed a lower fraction (3 % of

302   Arctic surface BC) (Fig. 5b). Few biomass-burning sources contributed in January (Fig. 5c),

303   but contributions from biomass burning to Arctic surface BC in July can be clearly seen,

304   mainly from the far east of Russia, Canada, and Alaska (Fig. 5d). Biomass burning emissions

305   from Kazakhstan, southwest Russia, southern Siberia, and northeast China also contributed

306   to Arctic surface BC, although at relatively low strengths (Fig. 5d and Fig. S1d). However, the

307   contributions from biomass burning could be higher, as the MODIS burned area, the basis of

308   GFED emission inventories, was underestimated for northern Eurasia by 16 % (Zhu et al.,

309   2017). Evangeliou et al. (2016) estimated a relatively high transport efficiency of BC from

310   biomass-burning emissions to the Arctic, which led to a high contribution, i.e., 60 %, from

311   such sources to BC deposition in the Arctic in 2010. A recent study suggested that open fires

312   burned in western Greenland in summer (31 July to 21 August 2017) could potentially alter

313   the Arctic air composition and foster glacier melting (Evangeliou et al., 2019). Although the

314   footprint of Arctic surface BC showed a relatively weak sensitivity to areas such as forests

315   and tundra, in the boreal regions, pollutants from boreal wildfires could have greater effects

316   on the Arctic air composition in summer under future warming scenarios (Veira et al., 2016).

317   **3.4 Sources of Arctic BC at high altitudes**

318   Arctic BC levels at high altitudes (4750–4250 m) showed the highest levels in spring

319   (March–April, 40.5–53.9 ng m^{-3}), followed by those in late autumn to early winter

320   (November–January, 36.5–40.0 ng m^{-3}), and summer (July–August, 33.0–39.0 ng m^{-3}) (Fig.

321   4). The annual mean Arctic BC at high altitudes was estimated to be 35.2 ng m^{-3}, which is ca.

322   73 % of those at the surface. Such a vertical profile is in accordance with those based on

323   aircraft measurements over the High Canadian Arctic (Schulz et al., 2019). Similarly to the

324   case for the surface, anthropogenic sources accounted for 94–100 % of Arctic BC at high

325   altitudes in October–May. East Asia accounted for 34–65 % of the total BC in October–May

326   (40 % annually). In comparison, using the Community Atmosphere Model version 5 driven

327   by the NASA Modern Era Retrospective-Analysis for Research and Applications reanalysis

328   data and the IPCC AR5 year 2000 BC emission inventory, H. Wang et al. (2014) found that

329   East Asia accounted for 23% of BC burden in the Arctic for 1995–2005. In summer, biomass

330   burning in the boreal regions accounted for 40–72 % (57 % on average) of Arctic BC at high

331   altitudes, similar to the source contributions to Arctic surface BC. Specifically, biomass-

332   burning sources from Siberia accounted for 40–42 % of Arctic BC at high altitudes in July–

333   August. Annually, anthropogenic sources and biomass burning accounted for 83 % and 17 %,

334   respectively, of total Arctic BC at high altitudes.

335   Further investigations of geospatial contributions to Arctic BC at high altitudes in January

336   and July provided more details regarding BC sources. In January, the main anthropogenic BC

337   source in East Asia covered a wide range in China (Fig. 5a). Not only east and northeast

338   China, but also southwest China (Sichuan and Guizhou provinces) were the major

339   anthropogenic sources of Arctic BC at high altitudes. In July, anthropogenic sources made a

340   relatively weak contribution to Arctic BC at high altitudes. The regions that were sources of

341   biomass-burning contributions to Arctic BC at high altitudes were mainly the far east of

342   Siberia, Kazakhstan, central Canada, and Alaska, i.e., similar to the sources of Arctic surface

343   BC. Unlike Arctic surface BC, for which the dominant source regions are at high latitudes in

344   both winter and summer, Arctic BC at high altitudes mainly originates from mid-latitude

345   regions (Figs. 5 and 6). In terms of transport pathways, air masses could be uplifted at low-

346   to-mid latitudes and transported to the Arctic (Stohl, 2006). Further investigations are

347   needed to obtain more details of the transport processes.

348   **3.5 Comparison of Flexpart and GEOS-Chem simulations of BC sources**

349   Data for BC sources simulated with Flexpart were compared with those obtained with

350   GEOS-Chem (Ikeda et al., 2017), which is an Eulerian atmospheric transport model, using the

351   same emission inventories. The simulated seasonal variations in Arctic BC levels and source

352   contributions obtained with Flexpart agreed well with those obtained with GEOS-Chem (Fig.

353   S3). The annual mean BC levels at the Arctic surface obtained by Flexpart and GEOS-Chem

354   simulations were 48 and 70 ng m^{-3}, respectively; the high-altitude values simulated by

355   Flexpart and GEOS-Chem were 35 and 38 ng m^{-3}, respectively. The magnitude difference

356   between the BC levels at the Arctic surface could be related to meteorology. ECMWF ERA-

357   Interim data were used as the input for the Flexpart simulation, whereas the GEOS-Chem

358   simulation was driven by assimilated meteorological data from the Goddard Earth

359   Observation System (GEOS-5).

360   The treatments of the BC removal processes could also lead to different simulation

361   results, depending on the model. In terms of BC loss processes, dry and wet depositions

362   were the removal pathways, depending on the particle size and density, in Flexpart. The

363   treatment of meteorology, especially cloud water and precipitation, would therefore affect

364   the uncertainties of the simulations. In Flexpart version 10.1, BC particles are separately

365   parameterized as ice nuclei for ice clouds, cloud condensation nuclei for liquid-water clouds,

366   and 90 % as cloud condensation nuclei for mixed-phase clouds. The separation of mixed-

367   phase clouds is realistic, as 77 % of in-cloud scavenging processes occurred in the mixed

368   phase over a 90 day period starting from December 2006 (Grythe et al., 2017).

369   In GEOS-Chem simulations, the BC aging was parameterized based on the number

370   concentration of OH radicals (Liu et al., 2011). The BC was assumed to be hydrophilic in

371   liquid clouds ($T \geq 258$ K) and hydrophobic when serving as ice nuclei in ice clouds ($T < 258$ K)

372   (Wang et al., 2011), with modifications because the scavenging rate of hydrophobic BC was

373   reduced to 5 % of water-soluble aerosols for liquid clouds (Bourgeois and Bey, 2011). Such a

374   treatment is expected to improve the simulation accuracy (Ikeda et al., 2017).

375   In Lagrangian models, the trajectories of particles are computed by following the

376   movement of air masses with no numerical diffusion, although some artificial numerical

377   errors could be generated from stochastic differential equations (Ramli and Esler, 2016). As

378   a result, long-range transport processes can be well simulated (Stohl, 2006; Stohl et al.,

379   2013). In comparison, Eulerian chemical transport models such as GEOS-Chem have the

380   advantage of simulating non-linear processes on the global scale, which enables treatment

381   of the BC aging processes (coating with soluble components) (Bey et al, 2001; Eastham et

382   al., 2018). However, with GEOS-Chem, the capture of intercontinental pollution plumes is

383   difficult because of numerical plume dissipation (Rastigejev et al., 2010). Nevertheless, the

384   agreement between the Flexpart and GEO-Chem simulations of BC source contributions

385   indicates improved reliability of evaluated source contributions to Arctic BC.

386   **4   Conclusions**

387   The source contributions to Arctic BC were investigated by using a Flexpart (version 10.1)

388   transport model that incorporated emission inventories. Flexpart-simulated BC data agreed

389   well with observations at Arctic sites, i.e., Barrow, Alert, Zeppelin, and Tiksi. The source

390   regions and source sectors of BC at the surface and high altitudes (~ 5000 m) over a wide

391   region in the Arctic north of 66° N were simulated. BC at the Arctic surface was sensitive to

392   local emissions and those from nearby Nordic countries (>60° N). These results emphasize

393   the role of anthropogenic emissions such as gas flaring and development of the Northern

394   Sea Route in affecting air quality and climate change in the Arctic. Anthropogenic emissions

395   in the northern regions of Russia were the main source (56 %) of Arctic surface BC annually.

396   In contrast, BC in the Arctic at high altitudes was sensitive to mid-latitude emissions (30–60°

397   N). Although they are geospatially far from the Arctic, anthropogenic emissions in East Asia

398   made a notable (40 %) contribution to BC in the Arctic at high altitudes annually. Biomass-

399 burning emissions, which were mainly from Siberia, Alaska, and Canada, were important in

400 summer, contributing 56–85 % of BC at the Arctic surface, and 40–72 % at Arctic high

401 altitudes. Future increases in wildfires as a result of global warming could therefore increase

402 the air pollution level during the Arctic summer. This study clarifies the source regions and

403 sectors of BC in the Arctic. This information is fundamental for understanding and tackling

404 air pollution and climate change in the region.

405

406 *Data Availability.* The data set for simulated footprint and BC source contributions is

407 available on request to the corresponding author.

408

409 *Author contributions.* CZ and YK designed the study. CZ, MT, and IP optimized the Flexpart

410 model. CZ performed Flexpart model simulations, conducted analyses, and wrote the

411 manuscript. KI and HT provided data for GEOS-Chem simulations and site observations. All

412 authors made comments that improved the paper.

413

414 *Competing interests.* The authors declare that they have no conflict of interest.

415 *Financial Support.* This study was supported by the Environmental Research and Technology

416 Development Fund (2-1505) of the Ministry of the Environment, Japan.

417

418 *Acknowledgment.* We thank Helen McPherson, PhD, from Edanz Group

419 (www.edanzediting.com/ac) for editing a draft of this manuscript.

420

421 **References**

422 AMAP Assessment 2015: Black carbon and ozone as Arctic climate forcers, Arctic Monitoring

423  and Assessment Programme (AMAP), Oslo, Norway, 2015.

424   Bey, I., Jacob, D. J., Yantosca, R. M., Logan, J. A., Field, B. D., Fiore, A. M., Li, Q. B., Liu, H. G.

425   Y., Mickley, L. J., and Schultz, M. G.: Global modeling of tropospheric chemistry with

426   assimilated meteorology: Model description and evaluation, J Geophys Res-Atmos, 106,

427   23073-23095, doi:10.1029/2001jd000807, 2001.

428   Bourgeois, Q. and Bey, I.: Pollution transport efficiency toward the Arctic: sensitivity to

429   aerosol scavenging and source regions, J. Geophys. Res., 116, D08213,

430   doi:10.1029/2010JD015096, 2011.

431   Brock, C. A., Cozic, J., Bahreini, R., Froyd, K. D., Middlebrook, A. M., McComiskey, A.,

432   Brioude, J., Cooper, O. R., Stohl, A., Aikin, K. C., de Gouw, J. A., Fahey, D. W., Ferrare, R.

433   A., Gao, R. S., Gore, W., Holloway, J. S., Hubler, G., Jefferson, A., Lack, D. A., Lance, S.,

434   Moore, R. H., Murphy, D. M., Nenes, A., Novelli, P. C., Nowak, J. B., Ogren, J. A., Peischl, J.,

435   Pierce, R. B., Pilewskie, P., Quinn, P. K., Ryerson, T. B., Schmidt, K. S., Schwarz, J. P.,

436   Sodemann, H., Spackman, J. R., Stark, H., Thomson, D. S., Thornberry, T., Veres, P., Watts,

437   L. A., Warneke, C., and Wollny, A. G.: Characteristics, sources, and transport of aerosols

438   measured in spring 2008 during the aerosol, radiation, and cloud processes affecting

439   Arctic Climate (ARCPAC) Project, Atmospheric Chemistry and Physics, 11, 2423-2453,

440   doi:10.5194/acp-11-2423-2011, 2011.

441   Cohen, J., Screen, J. A., Furtado, J. C., Barlow, M., Whittleston, D., Coumou, D., Francis, J.,

442   Dethloff, K., Entekhabi, D., Overland, J., and Jones, J.: Recent Arctic amplification and

443   extreme mid-latitude weather, Nature Geoscience, 7, 627-637, doi:10.1038/Ngeo2234,

444   2014.

445   Cozic, J., Verheggen, B., Mertes, S., Connolly, P., Bower, K., Petzold, A., Baltensperger, U.,

446   and Weingartner, E.: Scavenging of black carbon in mixed phase clouds at the high alpine

447   site Jungfraujoch, Atmos. Chem. Phys., 7, 1797-1807, doi:10.5194/acp-7-1797-2007,

448   2007.

449   Dong, X., Zhu, Q., Fu, J. S., Huang, K., Tan, J., and Tipton, M.: Evaluating recent updated black

450   carbon emissions and revisiting the direct radiative forcing in Arctic, Geophysical

451   Research Letters, 46, 3560– 3570. doi:10.1029/2018GL081242, 2019.

452   Eastham, S. D., Long, M. S., Keller, C. A., Lundgren, E., Yantosca, R. M., Zhuang, J. W., Li, C.,

453   Lee, C. J., Yannetti, M., Auer, B. M., Clune, T. L., Kouatchou, J., Putman, W. M., Thompson,

454   M. A., Trayanov, A. L., Molod, A. M., Martin, R. V., and Jacob, D. J.: GEOS-Chem High

455   Performance (GCHP v11-02c): a next-generation implementation of the GEOS-Chem

456   chemical transport model for massively parallel applications, Geosci Model Dev, 11,

457   2941-2953, doi:10.5194/gmd-11-2941-2018, 2018.

458 Eckhardt, S., Quennehen, B., Olivie, D. J. L., Berntsen, T. K., Cherian, R., Christensen, J. H.,

459   Collins, W., Crepinsek, S., Daskalakis, N., Flanner, M., Herber, A., Heyes, C., Hodnebrog,

460   O., Huang, L., Kanakidou, M., Klimont, Z., Langner, J., Law, K. S., Lund, M. T., Mahmood,

461   R., Massling, A., Myriokefalitakis, S., Nielsen, I. E., Nojgaard, J. K., Quaas, J., Quinn, P. K.,

462   Raut, J. C., Rumbold, S. T., Schulz, M., Sharma, S., Skeie, R. B., Skov, H., Uttal, T., von

463   Salzen, K., and Stohl, A.: Current model capabilities for simulating black carbon and

464   sulfate concentrations in the Arctic atmosphere: a multi-model evaluation using a

465   comprehensive measurement data set, Atmospheric Chemistry and Physics, 15, 9413-

466   9433, doi:10.5194/acp-15-9413-2015, 2015.

467 Evangeliou, N., Balkanski, Y., Hao, W. M., Petkov, A., Silverstein, R. P., Corley, R., Nordgren,

468   B. L., Urbanski, S. P., Eckhardt, S., Stohl, A., Tunved, P., Crepinsek, S., Jefferson, A.,

469   Sharma, S., Nojgaard, J. K., and Skov, H.: Wildfires in northern Eurasia affect the budget of

470   black carbon in the Arctic - a 12-year retrospective synopsis (2002-2013), Atmospheric

471   Chemistry and Physics, 16, 7587-7604, doi:10.5194/acp-16-7587-2016, 2016.

472 Evangeliou, N., Kylling, A., Eckhardt, S., Myroniuk, V., Stebel, K., Paugam, R., Zibtsev, S., and

473   Stohl, A.: Open fires in Greenland in summer 2017: transport, deposition and radiative

474   effects of BC, OC and BrC emissions, Atmospheric Chemistry and Physics, 19, 1393-1411,

475   doi:10.5194/acp-19-1393-2019, 2019.

476 Filimonova, I. V., Komarova, A. V., Eder, L. V., and Provornaya, I. V.: State instruments for the

477   development stimulation of Arctic resources regions, IOP Conference Series: Earth and

478   Environmental Science, 193, 012069, doi:10.1088/1755-1315/193/1/012069, 2018.

479 Garrett, T. J., Brattstrom, S., Sharma, S., Worthy, D. E. J., and Novelli, P.: The role of

480   scavenging in the seasonal transport of black carbon and sulfate to the Arctic,

481   Geophysical Research Letters, 38, L16805, doi:10.1029/2011gl048221, 2011.

482 Grythe, H., Kristiansen, N. I., Zwaaftink, C. D. G., Eckhardt, S., Strom, J., Tunved, P., Krejci, R.,

483   and Stohl, A.: A new aerosol wet removal scheme for the Lagrangian particle model

484   FLEXPART v10, Geosci Model Dev, 10, 1447-1466, doi:10.5194/gmd-10-1447-2017, 2017.

485 Hegg, D. A., Clarke, A. D., Doherty, S. J., and Ström, J.: Measurements of black carbon

486   aerosol washout ratio on Svalbard, Tellus B, 63, 891–900, doi:10.1111/j.1600-

487   0889.2011.00577.x, 2011.

488 Hertel, O., Christensen, J. Runge, E. H., Asman, W. A. H., Berkowicz, R., Hovmand, M. F., and
489   Hov, O.: Development and testing of a new variable scale air pollution model – ACDEP,
490   Atmos. Environ., 29, 1267–1290, 1995.
491 Hirdman, D., Burkhart, J. F., Sodemann, H., Eckhardt, S., Jefferson, A., Quinn, P. K., Sharma,
492   S., Strom, J., and Stohl, A.: Long-term trends of black carbon and sulphate aerosol in the
493   Arctic: changes in atmospheric transport and source region emissions, Atmospheric
494   Chemistry and Physics, 10, 9351-9368, doi:10.5194/acp-10-9351-2010, 2010.
495 Huang, K., and Fu, J. S.: A global gas flaring black carbon emission rate dataset from 1994 to
496   2012, Scientific Data, 3, 160104. doi:10.1038/sdata.2016.104, 2016.
497 Huang, K., Fu, J. S., Prikhodko, V. Y., Storey, J. M., Romanov, A., Hodson, E. L., Cresko, J.,
498   Morozova, I., Ignatieva, Y., and Cabaniss, J.: Russian anthropogenic black carbon:
499   Emission reconstruction and Arctic black carbon simulation, J Geophys Res-Atmos, 120,
500   11306-11333, doi:10.1002/2015jd023358, 2015.
501 Ikeda, K., Tanimoto, H., Sugita, T., Akiyoshi, H., Kanaya, Y., Zhu, C. M., and Taketani, F.:
502   Tagged tracer simulations of black carbon in the Arctic: transport, source contributions,
503   and budget, Atmospheric Chemistry and Physics, 17, 10515-10533, doi:10.5194/acp-17-
504   10515-2017, 2017.
505 Janssens-Maenhout, G., Crippa, M., Guizzardi, D., Dentener, F., Muntean, M., Pouliot, G.,
506   Keating, T., Zhang, Q., Kurokawa, J., Wankmüller, R., Denier van der Gon, H., Kuenen, J. J.
507   P., Klimont, Z., Frost, G., Darras, S., Koffi, B., and Li, M.: HTAP_v2.2: a mosaic of regional
508   and global emission grid maps for 2008 and 2010 to study hemispheric transport of air
509   pollution, Atmos. Chem. Phys., 15, 11411–11432, doi:10.5194/acp-15-11411-2015, 2015.
510 Keegan, K. M., Albert, M. R., McConnell, J. R., and Baker, I.: Climate change and forest fires
511   synergistically drive widespread melt events of the Greenland Ice Sheet, P Natl Acad Sci
512   USA, 111, 7964-7967, doi:10.1073/pnas.1405397111, 2014.
513 Kipling, Z., Stier, P., Schwarz, J. P., Perring, A. E., Spackman, J. R., Mann, G. W., Johnson, C.
514   E., and Telford, P. J.: Constraints on aerosol processes in climate models from vertically-
515   resolved aircraft observations of black carbon, Atmos. Chem. Phys., 13, 5969-5986,
516   doi:10.5194/acp-13-5969-2013, 2013.
517 Kirchstetter, T. W., Novakov, T., and Hobbs, P. V.: Evidence that the spectral dependence of
518   light absorption by aerosols is affected by organic carbon, J Geophys Res-Atmos, 109,
519   D21208, 10.1029/2004jd004999, 2004.

520 Klonecki, A., Hess, P., Emmons, L., Smith, L., Orlando, J., and Blake, D.: Seasonal changes in
521   the transport of pollutants into the Arctic troposphere-model study, J Geophys Res-
522   Atmos, 108, 8367, doi:10.1029/2002jd002199, 2003.

523 Koch, D., and Hansen, J.: Distant origins of Arctic black carbon: A Goddard Institute for Space
524   Studies ModelE experiment, J Geophys Res-Atmos, 110, D04204,
525   doi:10.1029/2004jd005296, 2005.

526 Lack, D. A., and Langridge, J. M.: On the attribution of black and brown carbon light
527   absorption using the Angstrom exponent, Atmospheric Chemistry and Physics, 13, 10535-
528   10543, doi:10.5194/acp-13-10535-2013, 2013.

529 Law, K. S., and Stohl, A.: Arctic air pollution: Origins and impacts, Science, 315, 1537-1540,
530   doi:10.1126/science.1137695, 2007.

531 Liu, J., Fan, S., Horowitz, L. W., and Levy II, H.: Evaluation of factors controlling long-range
532   transport of black carbon to the Arctic, J. Geophys. Res., 116, D00A14,
533   doi:10.1029/2010JD015145, 2011.

534 Liu, D., Quennehen, B., Darbyshire, E., Allan, J. D., Williams, P. I., Taylor, J. W., Bauguitte, S. J.
535   B., Flynn, M. J., Lowe, D., Gallagher, M. W., Bower, K. N., Choularton, T. W., and Coe, H.:
536   The importance of Asia as a source of black carbon to the European Arctic during
537   springtime 2013, Atmospheric Chemistry and Physics, 15, 11537-11555, doi:10.5194/acp-
538   15-11537-2015, 2015.

539 Ma, P.-L., Rasch, P. J., Wang, H., Zhang, K., Easter, R. C., Tilmes, S., Fast, J. D., Liu, X., Yoon, J.-
540   H., and Lamarque, J.-F.: The role of circulation features on black carbon transport into the
541   Arctic in the Community Atmosphere Model version 5 (CAM5), J. Geophys. Res.-Atmos.,
542   118, 4657–4669, doi:10.1002/jgrd.50411, 2013.

543 Najafi, M. R., Zwiers, F. W., and Gillett, N. P.: Attribution of Arctic temperature change to
544   greenhouse-gas and aerosol influences, Nature Climate Change, 5, 246-249,
545   doi:10.1038/Nclimate2524, 2015.

546 Park, R. J., Jacob, D. J., Palmer, P. I., Clarke, A. D., Weber, R. J., Zondlo, M. A., Eisele, F. L.,
547   Bandy, A. R., Thornton, D. C., Sachse, G. W., and Bond, T. C.: Export efficiency of black
548   carbon aerosol in continental outflow: Global implications, J Geophys Res-Atmos, 110,
549   D11205, doi:10.1029/2004jd005432, 2005.

550   Qi, L., Li, Q. B., Henze, D. K., Tseng, H. L., and He, C. L.: Sources of springtime surface black
551   carbon in the Arctic: an adjoint analysis for April 2008, Atmospheric Chemistry and
552   Physics, 17, 9697-9716, doi:10.5194/acp-17-9697-2017, 2017.
553   Quinn, P. K., Bates, T. S., Baum, E., Doubleday, N., Fiore, A. M., Flanner, M., Fridlind, A.,
554   Garrett, T. J., Koch, D., Menon, S., Shindell, D., Stohl, A., and Warren, S. G.: Short-lived
555   pollutants in the Arctic: their climate impact and possible mitigation strategies,
556   Atmospheric Chemistry and Physics, 8, 1723-1735, doi:10.5194/acp-8-1723-2008, 2008.
557   Ramli, H. M. and Esler, J. G.: Quantitative evaluation of numerical integration schemes for
558   Lagrangian particle dispersion models, Geosci. Model Dev., 9, 2441-2457,
559   doi:10.5194/gmd-9-2441-2016, 2016.
560   Rastigejev, Y., Park, R., Brenner, M., and Jacob, D.: Resolving intercontinental pollution
561   plumes in global models of atmospheric transport, J. Geophys. Res., 115, D02302,
562   doi:10.1029/2009JD012568, 2010.
563   Roiger, A., Thomas, J. L., Schlager, H., Law, K. S., Kim, J., Schafler, A., Weinzierl, B.,
564   Dahloktter, F., Krisch, I., Marelle, L., Minikin, A., Raut, J. C., Reiter, A., Rose, M., Scheibe,
565   M., Stock, P., Baumann, R., Bouapar, I., Clerbaux, C., George, M., Onishi, I., and Flemming,
566   J.: QUANTIFYING EMERGING LOCAL ANTHROPOGENIC EMISSIONS IN THE ARCTIC REGION
567   The ACCESS Aircraft Campaign Experiment, B Am Meteorol Soc, 96, 441-460,
568   doi:10.1175/Bams-D-13-00169.1, 2015.
569   Sand, M., Berntsen, T. K., von Salzen, K., Flanner, M. G., Langner, J., and Victor, D. G.:
570   Response of Arctic temperature to changes in emissions of short-lived climate forcers,
571   Nature Climate Change, 6, 286-289, doi:10.1038/Nclimate2880, 2016.
572   Schacht, J., Heinold, B., Quaas, J., Backman, J., Cherian, R., Ehrlich, A., Herber, A., Huang, W.
573   T. K., Kondo, Y., Massling, A., Sinha, P. R., Weinzierl, B., Zanatta, M., and Tegen, I.: The
574   importance of the representation of air pollution emissions for the modeled distribution
575   and radiative effects of black carbon in the Arctic, Atmos. Chem. Phys., 19, 11159–11183,
576   doi:10.5194/acp-19-11159-2019, 2019.
577   Schmale, J., Arnold, S. R., Law, K. S., Thorp, T., Anenberg, S., Simpson, W. R., Mao, J., and
578   Pratt, K. A.: Local Arctic Air Pollution: A Neglected but Serious Problem, Earths Future, 6,
579   1385-1412, doi:10.1029/2018ef000952, 2018.
580   Schulz, H., Zanatta, M., Bozem, H., Leaitch, W. R., Herber, A. B., Burkart, J., Willis, M. D.,
581   Kunkel, D., Hoor, P. M., Abbatt, J. P. D., and Gerdes, R.: High Arctic aircraft measurements

582   characterising black carbon vertical variability in spring and summer, Atmospheric

583   Chemistry and Physics, 19, 2361-2384, doi:10.5194/acp-19-2361-2019, 2019.

584   Sharma, S., Leaitch, W. R., Huang, L., Veber, D., Kolonjari, F., Zhang, W., Hanna, S. J.,

585   Bertram, A. K., and Ogren, J. A.: An evaluation of three methods for measuring black

586   carbon in Alert, Canada, Atmospheric Chemistry and Physics, 17, 15225-15243,

587   doi:10.5194/acp-17-15225-2017, 2017.

588   Shaw, G. E.: The arctic haze phenomenon, B Am Meteorol Soc, 76, 2403-2413, 1995.

589   Shen, Z. Y., Ming, Y., Horowitz, L. W., Ramaswamy, V., and Lin, M. Y.: On the Seasonality of

590   Arctic Black Carbon, J Climate, 30, 4429-4441, doi:10.1175/Jcli-D-16-0580.1, 2017.

591   Shindell, D. T., Chin, M., Dentener, F., Doherty, R. M., Faluvegi, G., Fiore, A. M., Hess, P.,

592   Koch, D. M., MacKenzie, I. A., Sanderson, M. G., Schultz, M. G., Schulz, M., Stevenson, D.

593   S., Teich, H., Textor, C., Wild, O., Bergmann, D. J., Bey, I., Bian, H., Cuvelier, C., Duncan, B.

594   N., Folberth, G., Horowitz, L. W., Jonson, J., Kaminski, J. W., Marmer, E., Park, R., Pringle,

595   K. J., Schroeder, S., Szopa, S., Takemura, T., Zeng, G., Keating, T. J., and Zuber, A.: A multi-

596   model assessment of pollution transport to the Arctic, Atmospheric Chemistry and

597   Physics, 8, 5353-5372, doi:10.5194/acp-8-5353-2008, 2008.

598   Sinha, P. R., Kondo, Y., Koike, M., Ogren, J. A., Jefferson, A., Barrett, T. E., Sheesley, R. J.,

599   Ohata, S., Moteki, N., Coe, H., Liu, D., Irwin, M., Tunved, P., Quinn, P. K., and Zhao, Y.:

600   Evaluation of ground-based black carbon measurements by filter-based photometers at

601   two Arctic sites, J Geophys Res-Atmos, 122, 3544-3572, doi:10.1002/2016jd025843,

602   2017.

603   Stohl, A., Forster, C., Frank, A., Seibert, P., and Wotawa, G.: Technical note: The Lagrangian

604   particle dispersion model FLEXPART version 6.2, Atmos. Chem. Phys., 5, 2461–2474,

605   doi:10.5194/acp-5-2461-2005, 2005.

606   Stohl, A.: Characteristics of atmospheric transport into the Arctic troposphere, J Geophys

607   Res-Atmos, 111, D11306, doi:10.1029/2005jd006888, 2006.

608   Stohl, A., Hittenberger, M., and Wotawa, G.: Validation of the Lagrangian particle dispersion

609   model FLEXPART against large-scale tracer experiment data, Atmos Environ, 32, 4245-

610   4264, doi:10.1016/S1352-2310(98)00184-8, 1998.

611   Stohl, A., Klimont, Z., Eckhardt, S., Kupiainen, K., Shevchenko, V. P., Kopeikin, V. M., and

612   Novigatsky, A. N.: Black carbon in the Arctic: the underestimated role of gas flaring and

613   residential combustion emissions, Atmospheric Chemistry and Physics, 13, 8833-8855,

614   doi:10.5194/acp-13-8833-2013, 2013.

615 Taketani, F., Miyakawa, T., Takashima, H., Komazaki, Y., Pan, X., Kanaya, Y., and Inoue, J.:

616   Shipborne observations of atmospheric black carbon aerosol particles over the Arctic

617   Ocean, Bering Sea, and North Pacific Ocean during September 2014, J Geophys Res-

618   Atmos, 121, 1914-1921, doi:10.1002/2015jd023648, 2016.

619 Tietze, K., Riedi, J., Stohl, A., and Garrett, T. J.: Space-based evaluation of interactions

620   between aerosols and low-level Arctic clouds during the Spring and Summer of 2008,

621   Atmospheric Chemistry and Physics, 11, 3359-3373, doi:10.5194/acp-11-3359-2011,

622   2011.

623 Tilling, R. L., Ridout, A., Shepherd, A., and Wingham, D. J.: Increased Arctic sea ice volume

624   after anomalously low melting in 2013, Nature Geoscience, 8, 643-646,

625   doi:10.1038/Ngeo2489, 2015.

626 Trusel, L. D., Das, S. B., Osman, M. B., Evans, M. J., Smith, B., Fettweis, X., McConnell, J. R.,

627   Noel, B. P. Y., and van den Broeke, M. R.: Nonlinear rise in Greenland runoff in response

628   to post-industrial Arctic warming, Nature, 564, 104-108, doi:10.1038/s41586-018-0752-4,

629   2018.

630 van der Werf, G. R., Randerson, J. T., Giglio, L., Collatz, G. J., Mu, M., Kasibhatla, P. S.,

631   Morton, D. C., DeFries, R. S., Jin, Y., and van Leeuwen, T. T.: Global fire emissions and the

632   contribution of deforestation, savanna, forest, agricultural, and peat fires (1997–2009),

633   Atmospheric Chemistry and Physics, 10, 11707-11735, doi:10.5194/acp-10-11707-2010,

634   2010.

635 Veira, A., Lasslop, G., and Kloster, S.: Wildfires in a warmer climate: Emission fluxes,

636   emission heights, and black carbon concentrations in 2090-2099, J Geophys Res-Atmos,

637   121, 3195-3223, doi:10.1002/2015jd024142, 2016.

638 Wang, H., Rasch, P. J., Easter, R. C., Singh, B., Zhang, R., Ma, P. L., Qian, Y., and Beagley, N.:

639   Using an explicit emission tag- ging method in global modeling of source-receptor

640   relationships for black carbon in the Arctic: Variations, Sources and Trans- port pathways,

641   J. Geophys. Res.-Atmos., 119, 12888–12909, doi:10.1002/2014JD022297, 2014.

642 Wang, Q., Jacob, D. J., Fisher, J. A., Mao, J., Leibensperger, E. M., Carouge, C. C., Le Sager, P.,

643   Kondo, Y., Jimenez, J. L., Cubison, M. J., and Doherty, S. J.: Sources of carbonaceous

644   aerosols and deposited black carbon in the Arctic in winter-spring: implications for

645 radiative forcing, Atmos. Chem. Phys., 11, 12453– 12473, doi:10.5194/acp-11-12453-

646 2011, 2011.

647 Wang, Q., Jacob, D. J., Spackman, J. R., Perring, A. E., Schwarz, J. P., Moteki, N., Marais, E. A.,

648 Ge, C., Wang, J., and Barrett, S. R. H.: Global budget and radiative forcing of black carbon

649 aerosol: constraints from pole-to-pole (HIPPO) observations across the Pacific, J.

650 Geophys. Res. Atmos., 119, 195–206, doi:10.1002/2013JD020824, 2014.

651 Winiger, P., Andersson, A., Eckhardt, S., Stohl, A., and Gustafsson, O.: The sources of

652 atmospheric black carbon at a European gateway to the Arctic, Nat Commun, 7, 12776,

653 doi:10.1038/ncomms12776, 2016.

654 Winiger, P., Barrett, T. E., Sheesley, R. J., Huang, L., Sharma, S., Barrie, L. A., Yttri, K. E.,

655 Evangeliou, N., Eckhardt, S., Stohl, A., Klimont, Z., Heyes, C., Semiletov, I. P., Dudarev, O.

656 V., Charkin, A., Shakhova, N., Holmstrand, H., Andersson, A., and Gustafsson, O.: Source

657 apportionment of circum-Arctic atmospheric black carbon from isotopes and modeling,

658 Sci Adv, 5, eaau8052, doi:10.1126/sciadv.aau8052, 2019.

659 Xu, J. W., Martin, R. V., Morrow, A., Sharma, S., Huang, L., Leaitch, W. R., Burkart, J., Schulz,

660 H., Zanatta, M., Willis, M. D., Henze, D. K., Lee, C. J., Herber, A. B., and Abbatt, J. P. D.:

661 Source attribution of Arctic black carbon constrained by aircraft and surface

662 measurements, Atmospheric Chemistry and Physics, 17, 11971-11989, doi:10.5194/acp-

663 17-11971-2017, 2017.

664 Yu, K., Keller, C. A., Jacob, D. J., Molod, A. M., Eastham, S. D., and Long, M. S.: Errors and

665 improvements in the use of archived meteorological data for chemical transport

666 modeling: an analysis using GEOS-Chem v11-01 driven by GEOS-5 meteorology, Geosci

667 Model Dev, 11, 305-319, doi:10.5194/gmd-11-305-2018, 2018.

668 Zhu, C., Kobayashi, H., Kanaya, Y., and Saito, M.: Size-dependent validation of MODIS

669 MCD64A1 burned area over six vegetation types in boreal Eurasia: Large underestimation

670 in croplands, Scientific reports, *7*, 4181, doi:10.1038/s41598-017-03739-0, 2017.

671
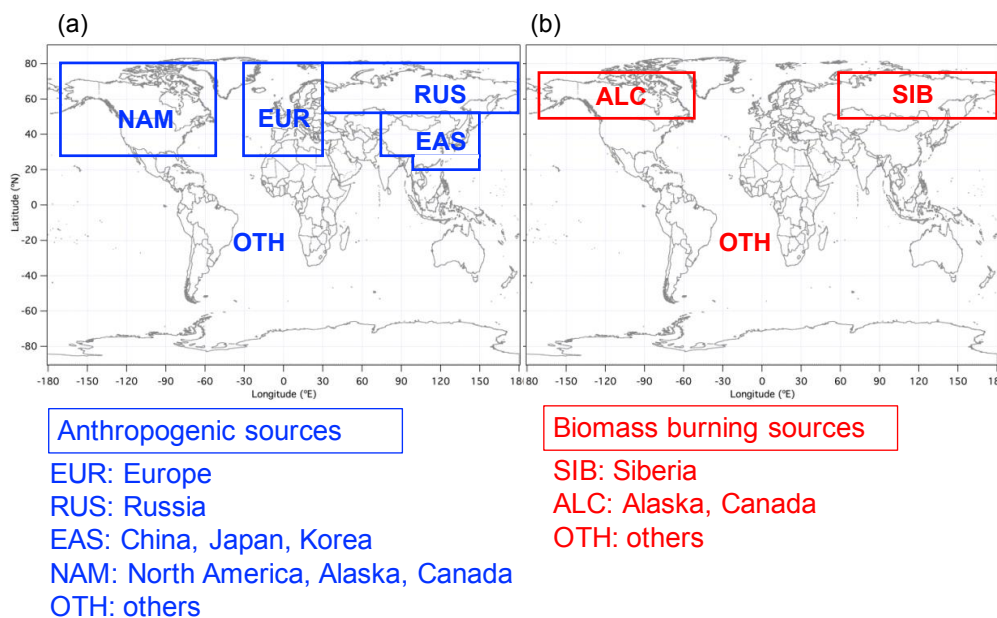
672

673 Figure 1. Regional separation for quantification of BC in the Arctic from (a) anthropogenic

674 and (b) biomass-burning sources.

675

676
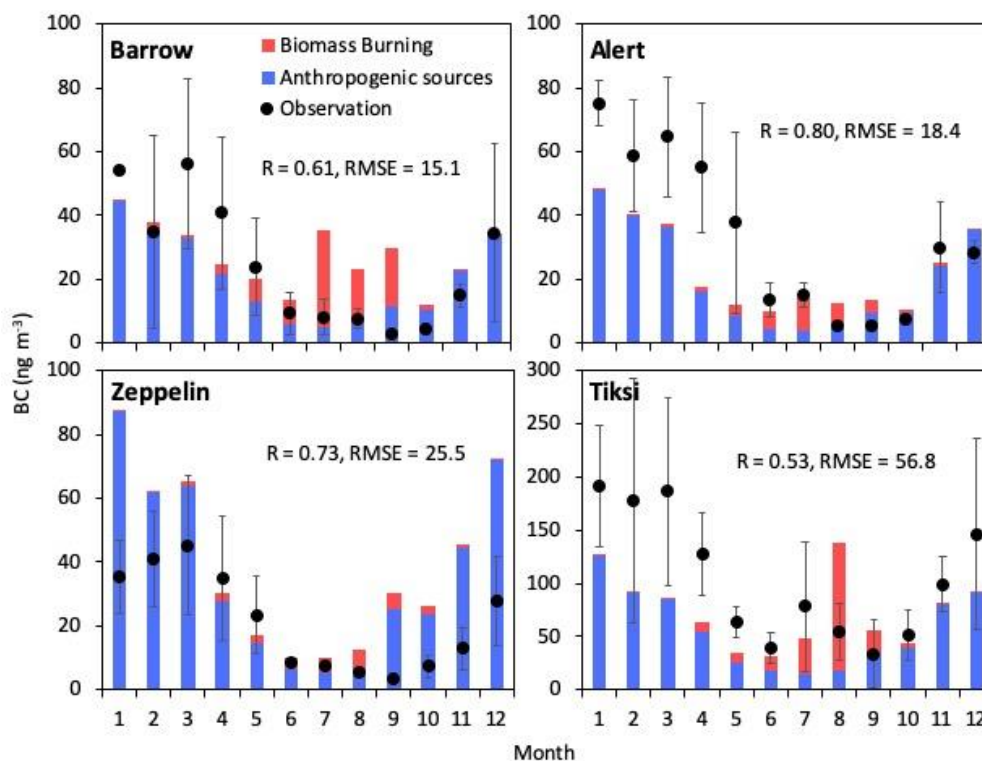
Figure 2. Observed (filled circles) and modeled (bars) seasonal variations in BC mass

concentrations at Arctic sites. Contributions from anthropogenic sources (blue) and biomass

burning (red) in each month are shown. Monthly averages of observed (filled circles) and

simulated (bars) BC were conducted for 2007–2011 at Barrow, USA (156.6° W, 71.3° N),

Alert, Canada (62.3° W, 82.5° N), and Zeppelin, Norway (11.9° E, 78.9° N), and for 2010–

2014 at Tiksi, Russia (128.9° E, 71.6° N). *R* and RMSE indicate correlation coefficient and

root-mean-square error (ng m^{-3}), respectively.

684

685
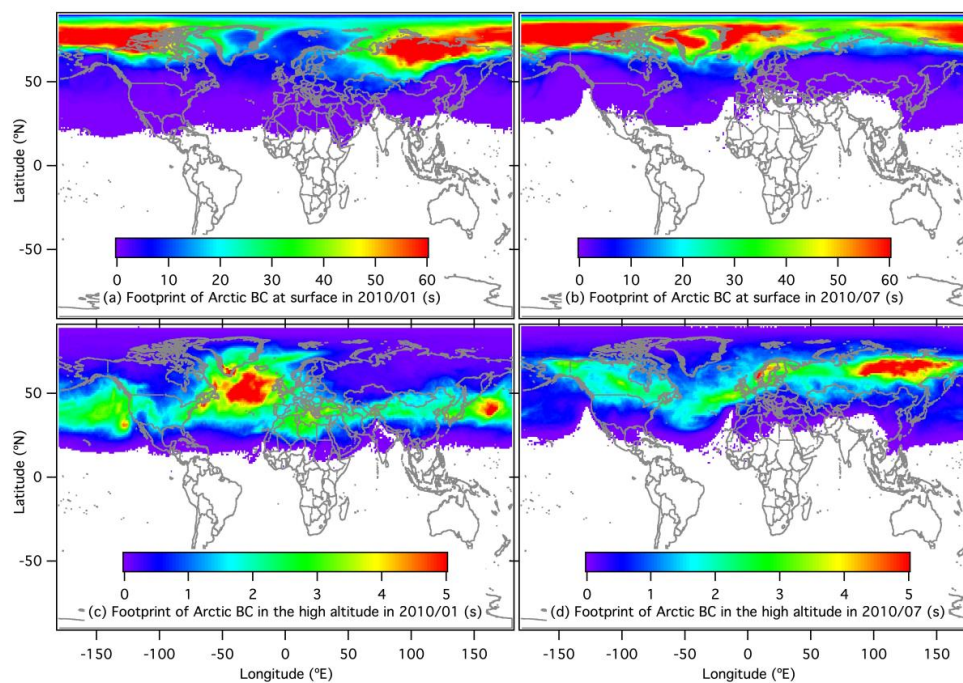
Figure 3. Footprints of Arctic BC shown as retention time(s) of (a) BC at surface (0–500 m) in

January 2010, (b) BC at surface in July 2010, (c) BC at high altitudes (4750–5250 m) in

January 2010, and (d) BC at high altitudes (4750–5250 m) in July 2010.

689
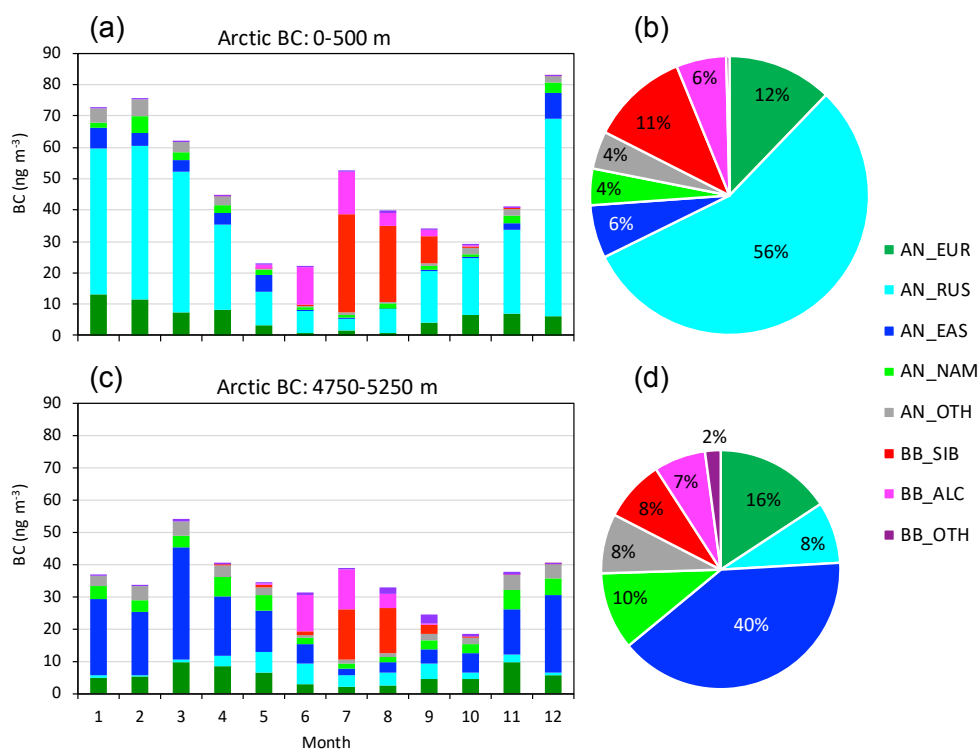
690
691 Figure 4. Contributions of anthropogenic sources and biomass burning from each region to

692 (a) seasonal variations in Arctic surface BC, (b) annual mean Arctic surface BC, (c) seasonal

693 variations in Arctic BC at high altitudes, and (d) annual mean of Arctic BC at high altitudes.

694

695
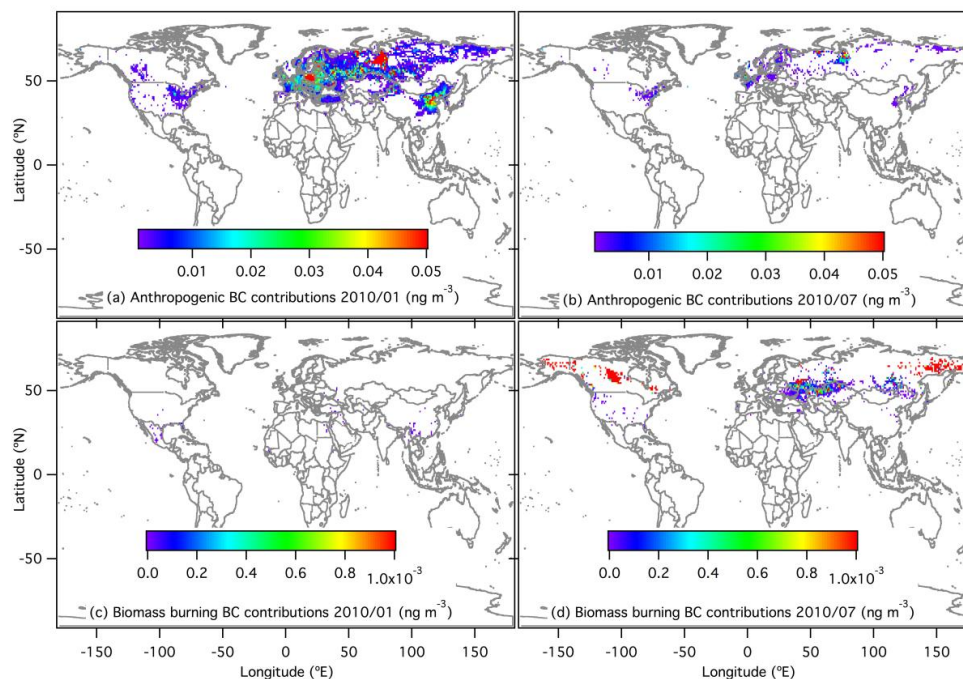
Figure 5. Spatial distributions of contributions to Arctic BC at surface (0–500 m) for (a)

anthropogenic contributions in January 2010, (b) anthropogenic contributions in July 2010,

(c) biomass-burning contributions in January 2010, and (d) biomass-burning contributions in

July 2010.

700

701
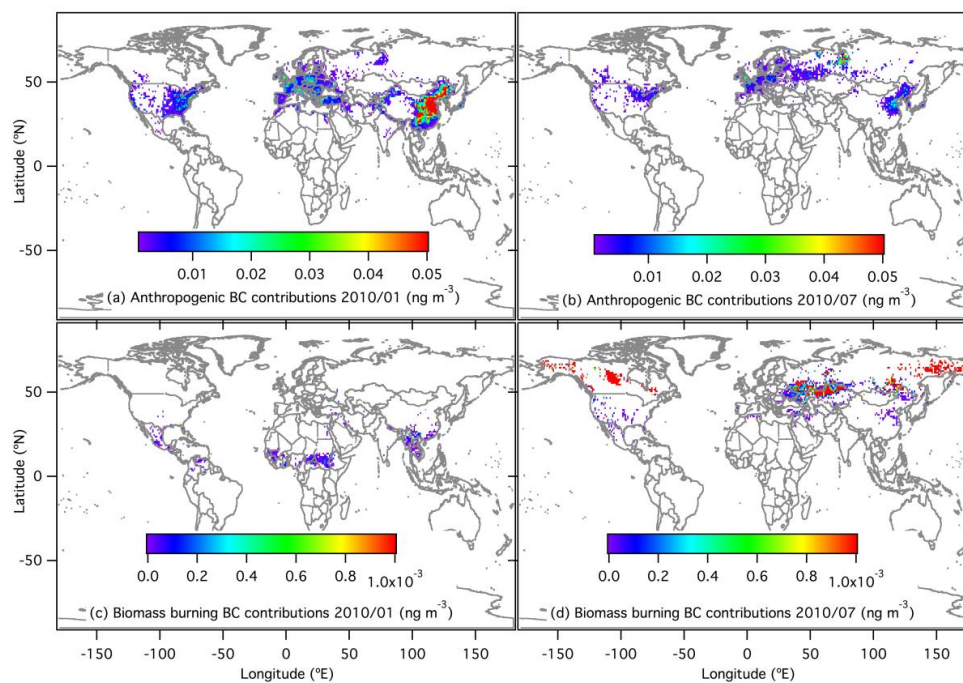
Figure 6. Spatial distributions of contributions to Arctic BC at high altitudes (4750–5250 m)

for (a) anthropogenic contributions in January 2010, (b) anthropogenic contributions in July

2010, (c) biomass-burning contributions in January 2010, and (d) biomass-burning

contributions in July 2010.

706